PCT

WORLD INTELLECTUAL PROPERTY ORGANIZATION
International Bureau

INTERNATIONAL APPLICATION PUBLISHED UNDER THE PATENT COOPERATION TREATY (PCT)

(51) International Patent Classification 6 : G02F 1/31	A1	(11) International Publication Number: WO 95/30924 (43) International Publication Date: 16 November 1995 (16.11.95)

(21) International Application Number: PCT/US95/05358

(22) International Filing Date: 1 May 1995 (01.05.95)

(30) Priority Data:
08/238,750 5 May 1994 (05.05.94) US

(60) Parent Application or Grant
(63) Related by Continuation
US 08/238,750 (CIP)
Filed on 5 May 1994 (05.05.94)

(71) Applicant (*for all designated States except US*): ETALON, INC. [US/US]; 33 Hanson Street, Boston, MA 02118 (US).

(72) Inventor; and
(75) Inventor/Applicant (*for US only*): MILES, Mark, W. [US/US]; 33 Hanson Street, Boston, MA 02118 (US).

(74) Agent: FEIGENBAUM, David, L.; Fish & Richardson P.C., 225 Franklin Street, Boston, MA 02110-2804 (US).

(81) Designated States: CA, CN, JP, KR, MX, US, European patent (AT, BE, CH, DE, DK, ES, FR, GB, GR, IE, IT, LU, MC, NL, PT, SE).

Published
With international search report.

(54) Title: VISIBLE SPECTRUM MODULATOR ARRAYS

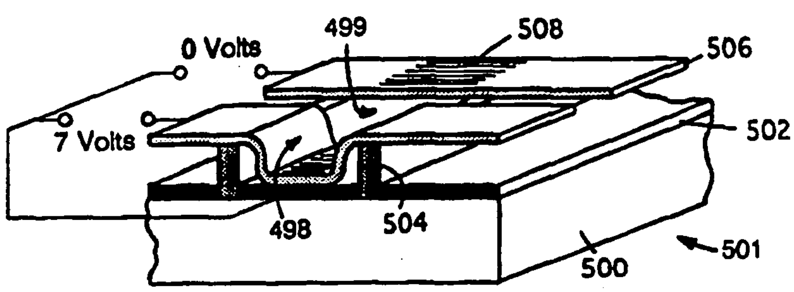

(57) Abstract

Light in the visible spectrum is modulated using an array of modulation elements (501), and control circuitry connected to the array for controlling each of the elements having a surface (506) which is caused to exhibit a predetermined impedance characteristic to particular frequencies of light. The amplitude of light delivered by each of the modulation elements is controlled independently by pulse code modulation. Each modulation element has a deformable portion (508) held under tensile stress, and the control circuitry controls the deformation of the deformable portion. Each deformable element has a deformation mechanism and an optical portion independently imparting to the element respectively a controlled deformation characteristic and a controlled modulation characteristic. The deformable modulation element may be a non-metal. The elements are made by forming a sandwich of two layers and a sacrificial layer between them, the sacrificial layer having a thickness related to the final cavity dimension, and using chemical (e.g., water) or a plasma based etch process to remove the sacrificial layer.

FOR THE PURPOSES OF INFORMATION ONLY

Codes used to identify States party to the PCT on the front pages of pamphlets publishing international applications under the PCT.

AT	Austria	GB	United Kingdom	MR	Mauritania
AU	Australia	GE	Georgia	MW	Malawi
BB	Barbados	GN	Guinea	NE	Niger
BE	Belgium	GR	Greece	NL	Netherlands
BF	Burkina Faso	HU	Hungary	NO	Norway
BG	Bulgaria	IE	Ireland	NZ	New Zealand
BJ	Benin	IT	Italy	PL	Poland
BR	Brazil	JP	Japan	PT	Portugal
BY	Belarus	KE	Kenya	RO	Romania
CA	Canada	KG	Kyrgystan	RU	Russian Federation
CF	Central African Republic	KP	Democratic People's Republic of Korea	SD	Sudan
CG	Congo			SE	Sweden
CH	Switzerland	KR	Republic of Korea	SI	Slovenia
CI	Côte d'Ivoire	KZ	Kazakhstan	SK	Slovakia
CM	Cameroon	LI	Liechtenstein	SN	Senegal
CN	China	LK	Sri Lanka	TD	Chad
CS	Czechoslovakia	LU	Luxembourg	TG	Togo
CZ	Czech Republic	LV	Latvia	TJ	Tajikistan
DE	Germany	MC	Monaco	TT	Trinidad and Tobago
DK	Denmark	MD	Republic of Moldova	UA	Ukraine
ES	Spain	MG	Madagascar	US	United States of America
FI	Finland	ML	Mali	UZ	Uzbekistan
FR	France	MN	Mongolia	VN	Viet Nam
GA	Gabon				

VISIBLE SPECTRUM MODULATOR ARRAYS

Background

This is a continuation-in-part of United States Patent Application Serial Number 08/238,750, filed May 5, 1994, which is a continuation-in-part of Serial No. 08/032,711, filed March 17, 1993.

This invention relates to visible spectrum (including ultra-violet and infrared) modulator arrays.

Visible spectrum modulator arrays, such as backlit LCD computer screens, have arrays of electro-optical elements corresponding to pixels. Each element may be electronically controlled to alter light which is aimed to pass through the element. By controlling all of the elements of the array, black and white or, using appropriate elements, color images may be displayed. Non-backlit LCD arrays have similar properties but work on reflected light. These and other types of visible spectrum modulator arrays have a wide variety of other uses.

Summary of the Invention

In general, in one aspect, the invention features modulation of light in the visible spectrum using an array of modulation elements, and control circuitry connected to the array for controlling each of the modulation elements independently, each of the modulation elements having a surface which is caused to exhibit a predetermined impedance characteristic to particular frequencies of light.

Implementations of the invention may include the following features. The surface may include antennas configured to interact with selected frequencies of light, or the surface may be a surface of an interference

cavity. The impedance characteristic may be reflection of particular frequencies of light, or transmission of particular frequencies of light. Each of the modulation elements may be an interference cavity that is deformable to alter the cavity dimension. The interference cavity may include a pair of cavity walls (e.g., mirrors) separated by a cavity dimension. One of the mirrors may be a broadband mirror and the other of the mirrors may be a narrow band mirror. Or both of the mirrors may be narrow band mirrors, or both of the mirrors may be broad band, non-metallic mirrors. The cavity may have a cavity dimension that renders the cavity resonant with respect to light of the frequency defined by the spectral characteristics of the mirrors and intrinsic cavity spacing in an undeformed state. One of the mirrors may be a hybrid filter. One (or both) of the walls may be a dielectric material, a metallic material, or a composite dielectric/metallic material. The cavity may be deformable by virtue of a wall that is under tensile stress. The control circuitry may be connected for analog control of the impedance to light of each element. The analog control may be control of the degree of deformity of the deformable wall of the cavity.

The predetermined impedance characteristic may include reflection of incident electromagnetic radiation in the visible spectrum, e.g., the proportion of incident electromagnetic radiation of a given frequency band that is, on average, reflected by each of the modulation elements. The modulation element may be responsive to a particular electrical condition to occupy either a state of higher reflectivity or a state of lower reflectivity, and the control circuitry may generate a stream of pulses having a duty cycle corresponding to the proportion of incident radiation that is reflected and places the modulation element in the higher state of reflectivity

during each the pulse and in the lower state of reflectivity in the intervals between the pulses. The characteristic may include emission of electromagnetic radiation in the visible spectrum. The characteristic may include the amount of electromagnetic radiation in the visible spectrum that is emitted, on average, by the antennas. The characteristic may be incident electromagnetic radiation in the visible spectrum. The modulation elements may include three sub-elements each associated with one of three colors of the visible spectrum. The modulation element may be responsive to a particular electrical condition to occupy either a state of higher transmissivity or a state of lower transmissivity, and the control circuitry may generate a stream of pulses having a duty cycle corresponding to the proportion of incident radiation that is transmitted and places the modulation element in the higher state of transmissivity during each the pulse and in the lower state of transmissivity in the intervals between the pulses. The characteristic may include the proportion of incident electromagnetic radiation of a given frequency band that is, on average, transmitted by each of the modulation elements.

The visible spectrum may include ultraviolet frequencies, or infrared frequencies.

In general, in another aspect of the invention, the control circuitry may be connected to the array for controlling the amplitude of light delivered by each of the modulation elements independently by pulse code modulation.

In general, in another aspect, the invention features a modulation element having a deformable portion held under tensile stress, and control circuitry connected to control the deformation of the deformable portion.

Implementations of the invention may include the following features. The modulation element may be self-supporting. or held on separate supports. The deformable portion may be a rectangular membrane supported along two opposite edges by supports which are orthogonal to the membrane. The deformable portion, under one mode of control by the control circuitry, may be collapsed onto a wall of the cavity. The control circuitry controls the deformable portion by signals applied to the modulation element, and the deformation of the control portion may be subject to hysteresis with respect to signals applied by the control circuitry.

In general, in another aspect, the invention features modulating light in the visible spectrum using a deformable modulation element having a deformation mechanism and an optical portion, the deformation mechanism and the optical portion independently imparting to the element respectively a controlled deformation characteristic and a controlled modulation characteristic.

Implementations of the invention may include the following features. The deformation mechanism may be a flexible membrane held in tensile stress, and the optical portion may be formed on the flexible membrane. The optical portion may be a mirror. The mirror may have a narrow band, or a broad band, or include a hybrid filter.

In general, in another aspect, the invention broadly features a non-metal deformable modulation element.

In general, in another aspect, the invention features a process for making cavity-type modulation elements by forming a sandwich of two layers and a sacrificial layer between them, the sacrificial layer having a thickness related to the final cavity dimension,

and using chemical (e.g., water) or a plasma based etch process to remove the sacrificial layer.

Among the advantages of the invention are the following.

Very high-resolution, full-color images are produced using relatively little power. The embodiment which senses the image incident on the array has relatively low noise. Their color response characteristics are tunable by selection of the dimensions of the antennas. The antenna or cavity embodiments are useful in portable, low power, full color displays, especially under high ambient light conditions. Phase controlled reflective embodiments are useful in passive light scanning such as optical disk readers without moving parts. The emissive embodiments also could be used as display devices especially in low-ambient-light conditions.

Because of the dielectric materials used in some embodiments, the devices have the advantage of being extremely light efficient, making them especially appropriate for high intensity projection displays, and reducing or eliminating the need for backlighting in low ambient light applications. In addition, more accurate color representations are possible, as well as designs optimized for the IR and UV. Mechanical hysteresis precludes the need for active drivers, and this coupled with their geometric simplicity and monolithic nature brings defect losses down significantly. The devices are also exceptionally fast, low power, and non-polarizing. The fact that they can be reflective and/or transmissive enhances their flexibility.

The process for fabrication as represented in some embodiments relies on benign chemicals, minimizing waste disposal problems, and facilitating the fabrication of devices on a variety of substrates (e.g., plastics or

integrated circuits) using a larger variety of materials. Devices on plastic substrates have the potential of being extremely inexpensive. All of the manufacturing technologies used are mature, further reducing manufacturing costs.

Other advantages and features of the invention will become apparent from the following description and from the claims.

Description

Fig. 1 is a perspective view of a display device.

Fig. 2 is a perspective schematic exploded view of a representative portion of the screen of Fig. 1.

Fig. 3 is an enlarged top view of a tri-dipole of Fig. 2.

Fig. 4 is a schematic view of a single dipole antenna of Fig. 3.

Fig. 5 is a schematic perspective view, broken away, of a portion of the screen of Fig. 1.

Fig. 6 is an enlarged top view of an individual tri-bus of Fig. 2.

Fig. 7 is an enlarged perspective view of a representative portion of the screen of Fig. 1.

Fig. 8 is a cross-sectional view along 8-8 of Fig. 7.

Fig. 9 is a diagram of a portion of a control circuit of Fig. 2, and a corresponding dipole antenna of Fig. 3.

Figs. 10A, 10B, 10C are representative graphs of the input voltage to the bias source of Fig. 9.

Fig. 11 is a diagram of portions of the control modules for a row of pixels,

Fig. 12 is a circuit diagram of an oscillator.

Fig. 13 is a schematic diagram of a circuit module of Fig. 2, a corresponding dipole antenna of Fig. 3, and

a graphical representation of the output of a binary counter.

Fig. 14 is a circuit diagram of the pulse counter of Fig. 13.

Figs. 15, 16, 17, 18, and 19 are top views of alternative dipole arrangements.

Figs. 20A through 20F are perspective views of a cavity devices.

Figs. 21A and 21B are side views of the cavity device.

Figs. 22A through 22F are graphs of useful pairs of frequency responses which can be achieved by the cavity device when it is in one of two states.

Figs. 22G through 22AF are a larger list of graphs of individual frequency responses which in some combinations prove useful in the cavity device.

Figs. 23A and 23B are top and cutaway side views respectively, of a display.

Figs. 23C and 23D are top and cutaway side views, respectively, of another display.

Fig. 23E is a side view of another display configuration.

Fig. 24A is a graph of an electromechanical response of the cavity device.

Figs. 24B and 24C are graphs of addressing and modulation schemes for a display.

Fig. 24D is a graph of a hysteresis curve.

Figs. 25A through 25N and Figs 26A through 26K are perspective views of the device during assembly.

Figs. 27A through 27C are side views of dielectric mirrors.

Fig. 27D is a top view of a dielectric mirror.

Figs. 28A, 28B are perspective and top views of a linear tunable filter.

Figs. 29A, 29B are perspective and top views of a deformable mirror.

Referring to Fig. 1, device 20 includes a screen 22 for displaying or sensing a high resolution color image (or a succession of color images) under control of power and control circuitry 26. The image is made up of a densely packed rectangular array of tiny individual picture elements (pixels) each having a specific hue and brightness corresponding to the part of the image represented by the pixel. The pixel density of the image depends on the fabrication process used but could be on the order of 100,000 pixels per square centimeter.

Referring to Fig. 2, each pixel is generated by one so-called tri-dipole 30. The boundary of each tri-dipole is T-shaped. The tri-dipoles are arranged in rows 32 in an interlocking fashion with the "Ts" of alternating tri-dipoles oriented in one direction and the "Ts" of intervening tri-dipoles along the same row oriented in the opposite direction. The rows together form a two-dimensional rectangular array of tri-dipoles (corresponding to the array of pixels) that are arranged on a first, external layer 34 of screen 22. The array may be called an electrically alterable optical planar array, or a visible spectrum modulator array.

On a second, internal layer 36 of screen 22 so-called tri-busses 38 (shown as T-shaped blocks in Fig. 2) are arranged in an interlocking two-dimensional array 40 corresponding to the layout of the tri-dipoles on layer 34 above. Each tri-dipole 30 is connected to its corresponding tri-bus 38 by a multi-conductor link 42 running from layer 34 to layer 36 in a manner described below.

On a third, base layer 44 of screen 22 a set of circuit modules 46 are arranged in a two-dimensional

rectangular array corresponding to the layouts of the tri-dipoles and tri-busses. Each circuit module 46 is connected to its corresponding tri-bus 38 by a six-conductor link 48 running from layer 36 to layer 44 in a manner described below.

Each circuit module 46 electronically controls the optical characteristics of all of the antennas of its corresponding tri-dipole 30 to generate the corresponding pixel of the image on screen 22. Circuit modules 46 are connected, via conductors 50 running along layer 44, to an edge of layer 44. Wires 52 connect the conductors 50 to control and power circuitry 26 which coordinates all of the circuit modules 46 to 25 generate the entire image.

Referring to Fig. 3, each tri-dipole 30 has three dipole sections 60, 62, 64. The center points 59, 61, 63 of the three sections are arranged at 120 degree intervals about a point 65 at the center of tri-dipole 30. Each section 60, 62, 64 consists of a column of dipole antennas 66, 68, 70, respectively, only ten dipole antennas are shown in each section in Fig. 3, but the number could be larger or smaller and would depend on, e.g., the density with which control circuits 46 can be fabricated, the tradeoff between bandwidth and gain implied by the spacing of the antennas, and the resistive losses of the conductors that connect the antennas to the control circuit 46. Only the two arms of each dipole antenna are exposed on layer 34, as shown in Fig. 3. The dipole antennas of a given section all have the same dimensions corresponding to a particular resonant wavelength (color) assigned to that section. The resonant wavelengths for the three sections 60, 62, 64 are respectively 0.45 microns (blue), 0.53 microns (green), and 0.6 microns (red).

Referring to Fig. 4, each dipole antenna 80 schematically includes two Ls 82, 84 respectively made up of bases 86, 88, and arms 90, 92. The bases of each antenna 80 are electrically connected to the corresponding circuit module 46. The span (X) of arms 90, 92 is determined by the desired resonant wavelength of dipole antenna 80; for example, for a resonant wavelength of lambda, X would be lambda/2. Dipole antennas 66, 68, 70 have X dimensions of 0.225 microns ($lambda_1$,/2), 0.265 microns ($lambda_2$/2), and 0.3 microns ($lambda_3$,/2), respectively. The effective length (Y) of bases 86, 88 from arms 90, 92 to circuit module 46 is also a function of the dipole antenna's resonant wavelength; for a resonant wavelength of lambda, Y is a multiple of lambda.

Referring to Fig. 5, each of the bases 86, 88 physically is made up of four segments; (1) one of the conductors 96 of link 42, (2) a portion 112 of tri-bus 38, (3) a short connecting portion 124 of tri-bus 38, and (4) one of the conductors 94 of link 48, which together define a path (e.g., the path shown as dashed line 97) with an effective length of Y from the arm (e.g., 92) to the circuit module 46.

The placement of link 42 perpendicular to the surface of layer 34 allows arms 90, 92 (formed on the surface of layer 34) to be spaced at an actual spacing Z that is closer than lambda/2, the minimum required effective Y dimension of bases 86, 88. Spacing Z may be chosen based on the bandwidth/gain tradeoff, and for example may be one quarter of the resonant wavelength for the dipole antennas of a given section (i.e., lambda/4, or 0.1125 microns ($lambda_1$/4), 0.1325 microns ($lambda_2$/4) and 0.15 microns ($lambda_3$/4) for antennas 66, 68, 70, respectively).

Referring to Fig. 6, each tri-bus 38 is formed of aluminum on layer 36 and has three zigzag shaped bus pairs 100, 102, 104 for respectively connecting dipole antennas of the corresponding sections 60, 62, 64 of tri-dipole 30. Bus pairs 100, 102, 104 are connected to individual dipole antennas 66, 68, 70 via conductors of link 42 (Fig. 2) that are joined to the bus pairs at points, e.g., 106.

Each bus pair 100, 102, 104 has two parallel buses 108, 110. Bus 108 electrically connects together the arms of the dipole antenna 5 of the corresponding section and, independently, the related bus 110 electrically connects together the arms 92 of the dipole antennas of that same section.

Points 106 delineate a series of fragments 112, 114, 116 on each of the three bus pairs 100, 102, 104, respectively. Each fragment forms part of one or more of the bases 86, or 88 and therefore contributes to the effective Y dimension.

The lengths (Q) of fragments 112, 114, 116 are one-half of the resonant wavelengths (i.e. lambda/2) of the sections 60, 62, 64, or 0.225 microns ($lambda_1$,/2), 0.265 microns ($lambda_2$,/2), and 0.3 microns ($lambda_3$,/2), respectively.

The conductors of link 48 (Fig. 2) are attached to tri-bus 38 at points 118, 120, 122 at the ends of buses 108, 110. Between points 118, 120, 122 and the first points 106 on along buses 108, 110 are fragments 124, 126, 128, which also form portions of the bases 86, 88 and are included to adjust the effective Y dimensions of those bases to be integer multiples of lambda/2. The lengths of the three fragments 124, 126, 128 are 0.1125 microns, 0.1525 microns, and 0.1875 microns, respectively.

Referring to Fig. 7, each dipole antenna 80 is physically formed (of aluminum) on an insulating semiconductor (e.g. silicon dioxide of silicon nitride) substrate 130 (part of layer 34) by x-ray or electron beam lithography or other technique suitable for forming submicron-sized structures.

Tri-busses 38 (not seen in Fig. 7) are formed on the upper-side of a second insulating semiconductor substrate 132 (part of layer 36). Circuit modules 46 (not seen in Fig. 7) are part of a third insulating semiconductor substrate 134 (part of layer 44) and are connected by conductors 50 to gold contact pads 136 (only one shown, not to scale) formed on the edge of substrate layer 134.

Referring to Fig. 8, circuit module 46 is formed in and on substrate 134 by any one of several monolithic processes. A section 138 of the substrate 134, which has been previously coated with an insulating semiconductor oxide layer 140, is repeatedly masked (whereby small windows are opened in the oxide layer, exposing the semiconductor beneath) and exposed to n and p dopants to form the desired circuit elements (not shown in detail in Fig. 8).

The individual circuit elements are connected to each other and to external contact pad 136 (Fig. 7) by aluminum conductors 142, 50, respectively. To form the connections, holes 144 are opened in oxide layer 140 and a sheet of aluminum is deposited, filling holes 144. Using a masking technique similar to the one described above the unwanted aluminum is removed, leaving only conductors 142, 50.

Semiconductor substrate layer 132 is deposited directly on top of the remaining exposed oxide layer 140 and conductors 142, 50. Holes 146 (one shown) (opened using a suitable lithographic technique) are channels for

the electrical conductors 147 of links 48, which connect tri-bus 38 and circuit module 46. Tri-bus 38 is etched from a sheet of aluminum deposited onto the surface of layer 132. The deposition process fills holes 146, thereby forming the conductors of links 48.

Substrate layer 130 is deposited onto the surface of substrate layer 132 and tri-bus 38. The arms of dipole antennas 80 are formed by depositing a sheet of aluminum onto the surface of layer 130 and etching away the unwanted metal. During the deposition process holes 148 are filled thereby forming the conductors 149 of links 42 between the arms of dipole antenna 80 and tri-bus 38.

The conductors 149 are the uppermost parts of bases 86, 88 (Fig. 4) of dipole antennas 66, 68, 70; the lengths of conductors 149 together with the lengths of fragments 112, 114, 116 (Fig. 6), the lengths of fragments 124, 126, 128, and the lengths of the conductors 147 determine the effective Y dimension of bases 86, 88.

The length of the conductors 149 is determined by the thickness of the substrate 130 through which links 42 pass. Substrate 130 and links 42 are 0.05625 microns (i.e. $lambda_1$,/8) thick. This thickness is achieved by controlling the deposition rate of the semiconductor material as layer 130 is formed.

The length of the conductors 149 is determined by the thickness of the substrate layer 132 through which they pass. This,layer and links 48 are therefore also 0.05625 microns 20 thick.

The Y dimensions for the dipole antennas 66, 68, 70 of sections 60, 62, 64 therefore are as follows:

(a) For section 60, Y equals the sum of 0.05625 microns (length of the conductor in link 42, $lambda_1/8$) + n * 0.225 microns (where 0.225 microns = $lambda_2/2$, the

length of a fragment 112, and n = the number of fragments 112 in each base 86, 88 of the nth dipole antenna 66n) + 0.1125 microns (length of fragment 124, $lambda_1/4$) + 0.05625 microns (length of the conductor in link 48, $lambda_1/8$), and that sum equals (n + 1) * ($lambda_{1/2}$).

(b) For section 62, Y equals the sum of 0.05625 microns (length of link 42, $lambda_1/8$) + n * 0.265 microns (where 0.265 microns = $lambda_2/2$, the length of a fragment 114, and n = the number of fragments 114 in each base 86, 88 of the nth dipole antenna 68n) + 0.1125 microns (length of fragment 126, ($lambda_2/2$) - ($lambda_1/4$)) + 0.05625 microns (length of the conductor in link 48, $lambda_1/8$), and that sum equals (n + 1)*($lambda_1/2$).

(c) For section 64, Y equals the sum of 0,05625 microns (length of conductor in link 42,$lambda_1/8$) + n * 0.3 microns (where 0.3 microns - $lambda_3/2$, the length of a fragment 116, and n equals the number of fragments 116 in each base 86, 88 of the nth dipole antenna 70n) + 0.1875 microns (the length of fragment 128, ($lambda_3/2$) - ($lambda_1/4$)) + 0.05625 microns (length of conductor in link 48), and that sum equals (n + 1) * ($lambda_3/2$).

Referring again to Fig. 1, in some embodiments, the displayed image is not emitted from device 20 but is comprised of ambient light (or light from a source, not 25 shown) selectively reflected by the tri-dipoles 30 of screen 22.

In that case, each tri-dipole 30 receives ambient light having a broad spectrum of wavelengths and is controlled by the corresponding circuit module to reflect only that portion of the ambient light manifesting the hue and brightness of the desired corresponding pixel.

The hue generated by tri-dipole 30 depends on the relative intensities of the light reflected by sections 60, 62, 64. The overall brightness of that hue of light

in turn depends on the absolute intensities of the light radiation reflected by sections 60, 62, 64. Thus, both the hue and brightness of the light generated by tri-dipole 30 can be controlled by regulating the intensity of the light reflected by the dipole antennas in each section of the tri-dipole; this is done by controlling the reflectivity of each dipole antenna, i.e.. the percentage of the light of the relevant wavelength for that dipole antenna which is reflected.

The desired percentage is attained not by regulating the amount of light reflected at any given instant but by arranging for the antenna to be fully reflective in each of a series of spaced apart time slots, and otherwise non-reflective. Each dipole antenna, in conjunction with its circuit module, has only two possible states: either it reflects all of the light (at the antenna's resonant frequency), or it reflects none of that light. The intensity is regulated by controlling the percentage of total time occupied by the time slots in which the dipole antenna occupies the first state.

Each dipole antenna is controlled to be reflective or not by controlling the impedance of the dipole antenna relative to the impedance of the medium (e.g., air) through which the light travels. If the medium has an effective impedance of zero, then the relationship of the reflectivity of the dipole antenna to zero (the controlled impedance of the dipole antenna) can be derived as follows. If we define a three-axis system x-y-z in which the x and y axes are in the plane of the array and the z axis is the axis of propagation of the incident and reflected waves, where z = 0 is the surface of the array, then the incident plus reflected wave for z < 0 may be represented as:

$$\overline{E} = \hat{x}E_0 e^{-jkz} + \hat{x}E_r e^{+jkz} \quad (1)$$

$$\overline{H} = \frac{\nabla\times\overline{E}}{-j\omega\mu_0} = \hat{y}\frac{1}{\eta_0}[E_0 e^{-jkz} - E_r e^{+jkz}] \quad (2)$$

where E (overbar) is the complex amplitude of the electric field of the sum of the transmitted wave and the reflected wave; E_0 is the complex amplitude of the electric field of the transmitted 20 wave; E_r, is the complex amplitude of the electric field of the reflective wave; x(hat) is the orientation of the electric field of the wave; H is the amplitude of the magnetic field; y(hat) is the orientation of the magnetic field; μo is the permeability of free space; ϵ_0 is the permittivity of free space; k = ωsqrt[$\mu_0\epsilon_0$] is the wavenumber; and η = sqrt [μ_0/ϵ_0] is the impedance of free space. For z > 0 (i.e.., within free space) only the transmitted wave exists and is represented by

$$\overline{E} = \hat{x}E_t e^{-jk_t z} \quad (3)$$

$$\overline{H} = \hat{y}\frac{1}{\eta_t}E_t e^{-jk_t z} \quad (4)$$

E(overbar) is the complex amplitude the transmitted wave at z = 0, k_t = sqrt [$\mu\epsilon$] is its wavenumber; η = sqrt [μ/ϵ] is the impedance of the medium, i.e. z > 0. Boundary conditions (z = 0) for tangential electric fields are imposed on equations 1 and 2 and they are combined to yield,

$$\hat{x}[E_0 + E_r] = \hat{x}E_t \quad (5)$$

In the same way, continuity for tangential magnetic fields (z = 0) at the boundary yields,
Dividing equations 5 and 6 by E_0, and E_0/η_0 respectively gives the following two equations:

$$\wp(1/\eta_0)(E_0-E_R) = \wp(1/\eta_t)E_t \tag{6}$$

$$1+E_r/E_0 = E_t/E_0 \tag{7}$$

$$1-E_R/E_0 = (\eta_0/\eta_t)(E_t/E_0) \tag{8}$$

E_r/E_0 is called Γ and is the complex reflection coefficient while E_t/η_0 = T is called the complex transmission coefficient, and $\eta_t/\eta_0 = \eta_n$ is the normalized wave impedance. Solving for T and Γ yields

$$T = \frac{E_t}{E_0} = \frac{2}{1+\eta_0/\eta_t} = \frac{2\eta_n}{\eta_n+1} \tag{9}$$

$$\Gamma = \frac{E_R}{E_0} = T-1 = \frac{\eta_N-1}{\eta_n+1} \tag{10}$$

For matched impedance values, $\eta_0 = \eta_n$, the reflection coefficient is zero, and T = 1 (i.e.., no reflection), and in the case of a load at the boundary, a matched antenna, there is complete absorption.

As η_n approaches zero or infinity, the reflection coefficient approaches plus or minus one, implying total reflection.

Referring to Fig. 9, the impedance z_L, of dipole antenna 80 is controlled by a variable resistance PIN diode 160 connected across bases 86, 88. PIN line 162 to the output of a bias high voltage or a low voltage based on a line 168 from power and the output of bias source 164 is a high voltage, the resistance R of PIN diode 160 (and hence the impedance (E,) of the dipole antenna is zero causing full reflection; when the output of bias source 164 is a low voltage 98, resistance R is set to a value such that the resulting impedance z@ is matched to z. (the impedance of the air surrounding the antenna), causing zero reflection.

To generate an entire image on screen 20, power and control circuitry 26 receives a video signal (e.g. a digitized standard RGB television signal) and uses conventional techniques to deliver corresponding signals to modules 46 which indicate the relative desired intensities of light reflected from all sections 60, 62, 64 of all of the tri-dipoles in the array at a given time. Circuit modules 46 use conventional techniques to deliver an appropriate stream of input control signal pulses to each bias source 164 on line 168.

The pulse stream on each line 168 has a duty cycle appropriate to achieve the proper percentages of reflectance for the three Sections of each tri-dipole. Referring to Figs. 10A, 10B, and 10C, for example, pulse stream 170 has a period T and a 50% duty cycle. For the first 50% of each period T the input to bias source 164 is high and the Corresponding output of source 164 is a high voltage. During this portion of the cycle dipole antenna 80 will reflect all received light having the dipole antenna's resonant wavelength. For the second 50% of the cycle the output of source 164 will be low and dipole antennas 80 will absorb the received light. In Figs. 10B, 10C, pulse streams 172, 174 represent a 30% duty cycle and a 100% duty cycle respectively; with a 30% duty cycle the effective intensity of the light radiation of the dipole antennas of the section will be 30%; for a duty cycle of 100%, the effective intensity is 100%.

For example, if a particular pixel of the image is to be brown, the relative intensities required of the three red, 25 green, and blue sections 60, 62, 64 may be, respectively, 30, 40, and 10. The input signals to the bias sources 164, carried on lines 168, would then have duty cycles, respectively, of 30%, 40%, and 10%. An adjacent pixel which is to be a brown of the same hue but

greater brightness might require duty cycles of 45%, 60%, and 15%.

Referring to Fig. 11, to accomplish the delivery of the pulse width modulated signals from circuitry 26 to the pixel circuit modules 46, each circuit module 46 in the row includes storage 180, 182 for two bits. The bit 1 storage elements 180 of the modules 46 in the row are connected together to create one long shift register with the pulse width modulated signals being passed along the row data line 184 from pixel to pixel. If, for example, the period of the modulated signals is 1 millisecond and there are ten different intensity levels, then an entire string of bits (representing the on or off state of the respective pixels in the row during the succeeding 1/10 millisecond) is shifted down the row every 1/10 millisecond. At the end of the initial 1/10 millisecond all of the bits in elements 180 are shifted to the associated elements 182 by a strobe Pulse on strobe line 186. The content of each element 182 is the input to the driver 188 for the appropriate one of the three colors of that pixel, which in turn drives the corresponding section 60, 62, 64 of the tri-dipole. The rate at which data is shifted along the shift registers is determined by the number of elements on a given row, the number of rows, the number of intensity levels, and the refresh rate of the entire array.

In another embodiment, the light comprising the image is emitted by tri-dipoles 30 rather than being produced by reflected ambient light. In that case, each tri-dipole generates the light for a single pixel with a hue and brightness governed by the intensities of the light emitted by each of the three sections 60, 62, 64.

Each dipole antenna within a tri-dipole is caused to emit light at the resonant wavelength of that antenna by stimulating it using a signal whose frequency

corresponds to the resonant wavelength. Thus, the sections 60, 62, 64 will emit blue ($lambda_1$), green ($lambda_2$), and red ($lambda_3$) light respectively when provided with signals whose frequencies equal, respectively, $lambda_1$, $lambda_2$ and $lambda_3$.

For an idealized dipole, the current I and current density J(overbar)(r'overbar) are described by

$$I = j\omega q \tag{11}$$

$$\bar{J}(\bar{r}') = \hat{z} I d \delta(\bar{r}') \tag{12}$$

where q is the charge density; z(hat) indicates the direction of the current (along the z-axis); ω is angular frequency; and d is the distance between ideal point charges representing the dipole. The vector potential A(overbar) in polar coordinates is given by

$$\begin{aligned}\bar{A} &= \hat{r}A_r + \hat{\theta}A_\theta \\ &= (\hat{r}\cos\theta - \hat{\theta}\sin\theta)\frac{\mu_0 I d}{4\pi r}e^{-jkr}\end{aligned} \tag{13}$$

where θ represents the angle relative to the dipole; θ(hat) is the angular orientation of the wave; μ_0 is the permeability of free space; r is radius from the dipole; r(hat) is radial orientation of the wave; A_r is the radial component of the vector potential; A_θ is the angular component of the vector potential; and k is a factor which is used to represent sinusoidally varying waves. The H field is given by

$$\begin{aligned}\bar{H} &= \varphi\frac{1}{\mu_0 r}\left[\frac{\delta}{\delta\theta}(rA_\theta - \frac{\delta}{\delta\theta}(A_r)\right] \\ &= \varphi\frac{jkId}{4\pi r}e^{-jkr}\left[1+\frac{1}{jkr}\right]\sin\theta\end{aligned} \tag{14}$$

where φ is elevation, with respect to the dipole. The E field is given by,

The far-field equation is given by

$$\bar{E} = \frac{1}{j\omega\epsilon_0}\nabla\times\bar{H}$$
$$= \sqrt{\mu_0/\epsilon_0}\frac{jkId}{4\pi r}e^{-jkr}(\hat{r}[\frac{1}{jkr}+(\frac{1}{jkr})^2]2\cos\theta \qquad (15)$$
$$+\hat{\theta}[1+\frac{1}{jkr}+(\frac{1}{jkr})^2]\sin\theta)$$

$$\bar{H} = \hat{\phi}\frac{jkId}{4\pi r}e^{-jkr}\sin\theta$$
$$\bar{E} = \hat{\theta}\sqrt{\mu_0/\epsilon_0}\frac{jkId}{4\pi r}e^{-jkr}\sin\theta \qquad (16)$$

Equation (16) describes the radiation pattern away from a dipole antenna at distances significantly greater than the wavelength of the emitted electromagnetic wave. It is a very broad radiation pattern providing a wide field of view at relevant distances.

Referring to Fig. 12, the dipole antennas 66, 68, 70 of each section 60, 62, 64 are driven by signals (e.g., sinusoidal) with frequencies of 5×10^{14} Hz, 5.6×10^{14} Hz, and 6.6×10^{14} Hz for red, green, and blue, respectively. These signals are supplied by three monolithic oscillators 200 (one shown) within circuit module 46, each tuned to one of the three required frequencies.

In circuit 200 (an a stable multivibrator), the center pair of coupled transistors 202, 204 are the primary active elements and will oscillate if the circuit admittance's are set appropriately. Diodes 206, 208, 210, 212 provide coupling capacitance's between the transistors and the inductors 214, 216 are used to tune the operating frequency.

In a third embodiment, an image of the object is focused by a conventional lens (not shown in Fig. 1) onto screen 22, which then acts as an image sensor. The tri-dipoles of screen 22, controlled by power and control circuitry 26, generate electrical signals corresponding

to pixels of the received image. The signals are then processed by a processor which, in conventional fashion, delivers a derived RGB video signal which can then be transmitted or stored.

The signals generated for each tri-dipole are generated by the corresponding circuit module 46 and represent the hue and brightness of the light radiation received at that tri-dipole.

Each section of tri-dipole 30 can only be used to measure light having the resonant wavelength of its respective dipole antennas, however, because most colors can be expressed as a combination of red, green, and blue, circuit module 46 can, by independently measuring the intensity of the light radiation received at each section 60, 62, 64, derive a signal which specifies the hue and intensity of the received pixel.

Referring to Fig. 13, dipole antenna 80 will absorb incident light radiation at its resonant wavelength when its reflection coefficient (Γ_L) is zero, which occurs when its controlled impedance (z_L) matches the impedance of the medium (z_0). In those circumstances, a voltage pulse is produced across the ends 308, 310 of dipole 80 for each incident photon. The relative magnitude of the light radiation received by each dipole antenna can thus be measured by counting the average number of pulses across ends 308, 310 over a given time period.

In this embodiment, circuit module 46 includes a terminating load resistor 315 connected across ends 308, 310. The controlled impedance of the combination of dipole antenna 80 and resistor 315, described by the equations set forth below, is equal to z_0.

The voltage of the pulse across resistor 315 (created by an incident photon) is illustrated by the

sine wave graph above register 15 and is described generally by the following equation

$$V(z) = \underline{V}{+}e^{-jkz}+\Gamma_L e^{jkz} \quad (17)$$

Because $z_L = z_0$, $\Gamma_L = 0$, and equation 17 simplifies to

$$V(z) = \underline{V}{+}e^{-jkz} \quad (18)$$

A pulse detector 318 amplifies and sharpens the resulting pulse to a square wave form as shown, which is then used as the clock (CLK) input 319 to a binary counter 320. The output of the binary counter is sampled at a regular rate; collectively the samples form a digital signal representing the intensity of received light radiation over time. Each time counter 320 is sampled, it is reset to zero by a pulse on control line 322, Counter 320 thus serves as a digital integrator that indicates how much light arrived in each one of a succession of equal length time periods.

Referring to Fig. 14, in pulse detector 318 the pair of transistors 322, 324 serve as a high impedance differential stage whose output (representing the voltage difference between points 308, 310) is delivered to an amplifier 326. Amplifier 326 serves as a high-bandwidth gain stage and delivers a single sided output pulse to a conditioning circuit 328 that converts slow rising pulses to square pulses 330 for driving counter 320.

In another embodiment, the array of tri-dipoles is operated as a phased array. The operation of phased arrays is discussed more fully in Amitay, et al., <u>Theory and Analysis of Phased Array Antennas</u>, 1972, incorporated herein by reference. By controlling the spacing of successive tri-dipoles across the array and the relative phases of their operation, wave cancellation or reinforcement can be used to control the direction in three dimensions and orientation of the radiation. Beams

can thus be generated or scanned. In the case of an array used to sense incoming radiation, the array can be made more sensitive to radiation received from selected directions.

Other embodiments are also possible. For example, referring to Fig. 15, each section of tri-dipole 400 array be a single dipole antenna 406, 407, 408. The tri-dipole antennas are then arranged about a center Point 410 at 120 degree intervals in a radial pattern. Bases 411, 412, as well as arms 414, 415, of the dipole antennas, are all formed on the same surface.

Referring to Fig. 16, each section may consist of multiple dipole antennas 406, 407, 408 connected by attaching the bases 411, 412 of each succeeding dipole antenna to the inner ends of arms 414, 415 of the preceding dipole antenna. Circuit modules 416 are formed on the surface of layer 413.

Referring to Fig. 17, a multi-dipole 430 could have five sections 432, 434, 436, 438, 440 composed of dipole antennas 442, 444, 446, 448, 450, respectively. The dipole antennas of the different sections would have different resonant wavelengths. Other multi-dipoles might have any number of sections.

The scanning of pixels could be done other than by pulse width modulation, for example, using charge coupled devices to shift packets of charge along the rows of pixels.

Referring to Figs. 18, 19, other arrangements of dipole antennas may be used in order to match the area required for the control circuit modules.

Referring to Fig. 18, each section 470 of a tri-dipole in the reflective mode could be formed of a number of subsections (e.g., 472) arranged in two rows 474 and a number of columns 47. The antennas 478 in each subsection 472 are all served by a single PIN diode

circuit 480 located at the peripheral edge of section 470 at the end of the subsection on the layer below the antenna layer. All circuits 480 for the entire Section 470 are in turn served by a single bias source 164 (Fig. 9). This arrangement reduces the number of bias sources required for the entire array of tri-dipoles. Fig. 19 shows an alternate arrangement in which there is but one row of subsections each ~~served by a single~~ PIN diode circuit at the end of the row.

In order to reduce the number of conductors 50, selected tri-dipoles could be used to receive control signals transmitted directly by light and to pass those control signals to the control circuits of nearby active tri-dipoles.

The dipoles could be mono-dipoles comprised of only a single dipole antenna, all with the same resonant wavelength.

Dipole antennas 470 could be randomly arranged on the surface of layer 472 of screen 22.

A different color regime, e.g. cyan-magenta-yellow, could be substituted for RGB.

Spiral, biconical, slotted, and other antenna configurations could be substituted for the dipole configuration.

The array could be three-dimensional.

The successive tri-dipoles in the array can be oriented so that their respective antennas are orthogonal to each other to enable the array to interact with radiation of any arbitrary polarization.

The PIN diodes could be replaced by other impedance controlling elements. Such elements might include quantum well transistors, superconducting junctions, or transistors based on vacuum microelectronics. Further improvement could be achieved by reducing the complexity of the third layer containing

control circuitry. The electronics required to get control signals to the circuitry could be eliminated by the use of laser or electron beams to provide such signals. This would have the advantage of allowing for arrays of even higher density.

The array could be fabricated on a transparent substrate, thus facilitating transmissive operation.

In other embodiments, ~~the antenna~~ arrays alone (without control circuitry or connection buses) may be fabricated on one-half of a microfabricated interferometric cavity. The antenna array can be considered a frequency selective mirror whose spectral characteristics are controlled by the dimensions of the antennas. Such a cavity will transmit and reflect certain portions of incident electromagnetic radiation depending on (a) the dimensions of the cavity itself and (b) the frequency response of the mirrors. The behavior of interferometric cavities and dielectric mirrors is discussed more fully in Macleod, H. A., Thin Film Optical Filters, 1969, incorporated by reference.

Referring to Fig. 20a, two example adjacent elements of a larger array of this kind include two cavities 498, 499 fabricated on a transparent substrate 500. A layer 502, the primary mirror/conductor, is comprised of a transparent conductive coating upon which a dielectric or metallic mirror has been fabricated. Insulating supports 504 hold up a second transparent conducting membrane 506. Each array element has an antenna array 508 formed on the membrane 506. The two structures, 506 and 508, together comprise the secondary mirror/conductor. Conversely, the antenna array may be fabricated as part of the primary mirror/conductor. Secondary mirror/conductor 506/508 forms a flexible membrane, fabricated such that it is under tensile stress

and thus parallel to the substrate, in the undriven state.

Because layers 506 and 502 are parallel, radiation which enters any of the cavities from above or below the array can undergo multiple reflections within the cavity, resulting in optical interference. Depending on the dimensions of the antenna array, as explained above, the interference will determine its ~~effective~~ impedance, and thus its reflective and/or transmissive characteristics. Changing one of the dimensions, in this case the cavity height (i.e., the spacing between the inner walls of layers 502, 506), will alter the optical characteristics. The change in height is achieved by applying a voltage across the two layers at the cavity, which, due to electrostatic forces, causes layer 506 to collapse. Cavity 498 is shown collapsed (7 volts applied), while cavity 499 is shown uncollapsed (0 volts applied).

In another embodiment, Fig. 20b, each cavity may be formed by a combination of dielectric or metallic mirrors on the two layers, and without the antennas formed on either layer. In this case the spectral characteristics of the mirror are determined by the nature and thickness(es) of the materials comprising it.

In an alternative fabrication scheme, Fig. 20c, each cavity is fabricated using a simpler process which precludes the need for separately defined support pillars. Here, each secondary mirror/conductor, 506, is formed in a U-shape with the legs attached to the primary layer; each secondary mirror/conductor thus is self-supporting.

In yet another scheme, Fig. 20d, the cavity has been modified to alter it's mechanical behavior. In this version, a stiffening layer, 510, has been added to limit deformation of the membrane while in the driven state. This assures that the two mirrors will remain parallel as

a driving voltage is gradually increased. The resulting device can be driven in analog mode (e.g., cavity 511 may be driven by 5 volts to achieve partial deformation of the cavity) so that continuous variation of its spectral characteristics may be achieved.

Figure 20E illustrates an additional configuration. In this scheme a stop layer 512 has been added so that the position of the membrane 506 in the driven state may be a fixed offset from the wall 502. Alternative optical, electrical, or mechanical responses may be accommodated in this fashion. For example, the stop layer may act as an insulator between walls 506 and 502, or its thickness may be set to achieve a certain center frequency when the device is driven.

Figure 20F shows an encapsulated version of the device of the cavity. Encapsulation membrane 514 is fabricated in the same fashion and using similar materials as the original cavity, 502 and 506 by use of the described processes. In this case, the process is used to build structures on top of an array of cavities which have already been fabricated. Encapsulation membrane 514 is a continuous structure designed to be rigid and inflexible. The function of this encapsulation is multifold. First it acts as a hermetic seal so that the entire array can be purged with an inert gas and maintained at an appropriate pressure. Second, the electrical and optical properties may also be useful in the overall operation of the array. Using electrically conducting materials, a voltage may be applied to encapsulation membrane 514, and the resulting electrostatic forces between membranes 514 and 506 can alter the hysteresis of the underlying cavity in a useful fashion. The collapse and release thresholds can be modified beyond what is dictated by the structure of the cavity itself. The electrostatic forces may also aid in